MISSOURI S&T

Missouri University of Science and Technology

Scholars' Mine

Physics Faculty Research & Creative Works

Physics

01 Nov 1993

Large-Cell Renormalization-Group Approach to Long-Range Hopping on Energetically Disordered Lattices

B. D. Bookout

Paul Ernest Parris
Missouri University of Science and Technology, parris@mst.edu

Follow this and additional works at: https://scholarsmine.mst.edu/phys_facwork

🄶 Part of the Physics Commons

Recommended Citation

Large-cell renormalization-group approach to long-range hopping on energetically disordered lattices

B. D. Bookout and P. E. Parris

Department of Physics and the Electronic Materials Institute, The University of Missouri–Rolla, Rolla, Missouri 65401

(Received 14 May 1993; revised manuscript received 15 July 1993)

We describe an approach for computing the conductivity associated with long-range hopping on energetically disordered lattices. Using a numerically exact supercell procedure we compute the distribution $\rho_L(\gamma)$ of block conductances γ_L associated with conducting cubes of edge length L that are randomly chosen from the disordered system of interest. This distribution of block conductances is then used in a self-consistent numerical calculation to obtain the renormalized bulk conductivity. The approach displays a surprisingly fast approach to the infinite-system limit, allowing finite-size effects to be minimized. In this paper we use this approach to study transport in a series of binary lattices containing a random distribution of two enegetically inequivalent ions. Specific examples considered include variations of the nearest-neighbor site percolation problem, long-range hopping on more general binary lattices, and the trapping-to-percolation transition that occurs in such systems.

I. INTRODUCTION

Electronic conduction in a large number of physical systems occurs as a result of the random hopping of charge carriers among a set of localized states possessing some degree of topological or energetic disorder. Important examples include transport between localized impurity states in doped semiconductors,[1–4] molecularly doped polymers and low-dimensional organic conductors,[5,6] molecular crystals,[7,8] and substitutionally mixed electronic ceramics.[9–11] Hopping transport is also an important mechanism for several uncharged species, examples of which include excited electronic energy transport (i.e., excitons), spin diffusion, vibrational energy transfer, and other quasi-particle-like excitations.[12–14] This makes the development of efficient procedures for computing transport coefficients for such systems an important task. As a consequence, a number of such procedures have been developed. Probably the most common approach involves the use of Monte Carlo simulations to randomly evolve the *position* of a transport particle as it executes a specific realization of the random walk in the appropriate random environment.[6,7,15] This is computationally efficient for nearest-neighbor walks, but is also extensible (with some limitations) to long-range hopping processes. Slightly less common are those approaches which employ a direct evolution of the site occupation *probabilities,* which are governed by an associated master equation. An advantage offered by this latter approach is that the evolving probabilities carry information about all possible random walks occurring in the system. This advantage, of course, occurs at the computational expense of having to evolve a more complicated and extensive set of quantities. As a practical consequence this means that one is usually restricted to performing computations of this latter type on smaller lattices than are generally possible if only the position of the particle is monitored. In some sense, therefore, the two methods are complementary.

In this paper we describe a computational approach for evaluating accurate transport coefficients associated with long- or short-range random walks on energetically disordered lattices. The approach incorporates the aforementioned advantages associated with an evolution of the probabilities, but uses large-cell renormalization-group ideas[16,18] to overcome the difficulties associated with the limited size of the lattices which can be considered computationally. Using supercell sizes having edge lengths L in the range of 4–6 lattice sites we have been able to reproduce the previously calculated conductivity for site-percolating networks, in which cubic regions having edge lengths of the order of 20 sites have proven necessary to obtain results which are reasonably free of finite-size effects.[2] We also present model calculations which explore the trapping-to-percolation crossover considered recently as an explanation for the conductivity minimum observed in substitutionally mixed small-polaron conducting ceramics.[9,10] Our numerical calculations confirm the essential features of this crossover and provide a test of recent approximate calculations based upon the authors' energy-projected effective-medium theory.[10] The rest of the paper is laid out as follows. In the next section we describe the general approach, which requires for its implementation the ability to compute the block conductance γ_L of cubic regions of a given fixed size L. In Sec. III we summarize a general method by which these block conductances may be obtained using a numerically exact spectral method,[11] which is computationally efficient for reasonably sized blocks. In Sec. IV we present model calculations intended to demonstrate the efficiency and accuracy of our method.

II. THE METHOD

The basic computational problem which we consider is one in which charge carriers in fractional site concentration n hop among the sites of a topologically ordered but energetically disordered d-dimensional cubic lattice (with

unit lattice spacing). The energetic disorder may arise, for example, due to the occupation of lattice sites by ions of several different species. We denote by x_μ the fraction of lattice sites occupied by ions of species μ and by ε_μ the energy associated with a charge carrier when it is located at a site containing an ion of this species. Equivalently, we can describe the distribution of site energies through a site energy distribution function $\Gamma(\varepsilon)$. A carrier at a given site m can, in principle, hop to any other site n in the lattice, with a hopping rate W_{nm}, which depends on distance, energy mismatch, and (for interacting particles) the probability that the site is already occupied. It has been noted in a number of theoretical treatments of this problem that the individual hopping rates between sites are random variables which can be viewed as (directed) microscopic *conductances* γ_{nm} connecting the nodes of a hypothetical random electrical network.[2,16] This observation has led to a whole class of approximate *analytical* treatments which seek to identify an (ordered) *effective-medium* network[2,12,17–21] in which perturbations due to embedded defects (i.e., random bonds or sites) of the type encountered in the actual disordered system self-consistently average out to zero. Approximate analytical procedures based upon this idea give surprisingly accurate estimates of the conductivity for nearest-neighbor networks, but tend to break down when the system under consideration is close to a critical point—an important concern in percolative systems.[2] Roughly speaking, such a breakdown can be expected to occur when the correlation length ξ significantly exceeds the size of the defect region which is averaged over in the approximate calculations. Moreover, extensions of effective-medium theory to the long-range hopping problem are less analytically tractable than in the case of nearest-neighbor systems.[10,21]

In our approach, we envision the actual disordered solid as being decomposed into a series of d-dimensional cubic regions or *blocks* having an edge length of L sites (we assume unit lattice spacing throughout), with each block containing a random configuration of $N = L^d$ ions with site energies chosen from the distribution $\Gamma(\varepsilon)$. With the ith block we associate a local conductance tensor γ_i, which governs the current flow through that block in response to electrical potential gradients imposed across its faces. For low fields this quantity depends both on the local equilibrium carrier concentration n_i and the Cartesian components D_i^ν of the local diffusion tensor associated with the carriers in that block. To proceed, we replace the original cubic network having unit lattice spacing with one whose lattice spacing is equal to the edge length L of the individual blocks originally considered, identifying the (now strictly nearest-neighbor) conductances coming out of the positive axis at each super-lattice point with the corresponding Cartesian components γ_i^ν of the associated block conductance tensor (see Fig. 1). This new system is intended to have the same bulk conductivity as the original. Moreover, for a sufficiently large block size the conductances associated with different blocks will be independent of one another, and can be taken as independently distributed random variables.
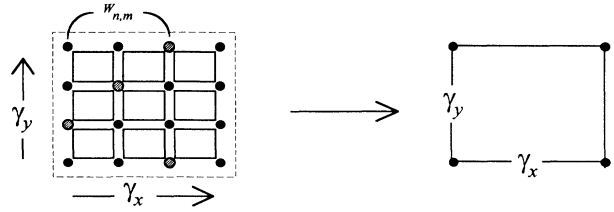

FIG. 1. Schematic illustration of the numerical renormalization process. Each disordered supercell containing L^d sites is replaced by a new unit cell containing a single site connected by equivalent conductances γ_i to its neighbors.

In a traditional renormalization-group approach the formal procedure outlined above would be analytically (although often only approximately) repeated on a larger length scale in an attempt to find a fixed point.[16,19] In practice, however, we can expect the distribution $\rho_L(\gamma_i)$ of block conductances obtained after a single decimation of the lattice to be both *smoother* and more *narrow* than the distribution $\rho_L(\gamma_{nm} = W_{nm})$ of microscopic conductances (or rates) connecting individual sites in the original system. This just reflects the fact that the homogeneity of a system depends upon the length scale at which it is examined. (Indeed, for a sufficiently *large* block size, the distribution will be sharp at the single value associated with the bulk conductivity.)

This natural smoothing of the distribution function leads us to reconsider the idea of employing an *effective-medium theory*, not at the length scale of an individual atomic site (as it is usually employed), but on a larger length scale for which it is expected to become more accurate. Thus, the bulk conductivity σ of a (renormalized) hypercubic lattice whose sites are connected by conductances drawn from an isotropic distribution $\rho_L(\gamma_i)$ is associated with that of a translationally invariant network in which nearest-neighbor sites are connected by a single *effective* conductance γ. Within the well-known coherent-potential approximation the appropriate conductance γ is identified with the root of a self-consistent equation[2,12,20,21]

$$\left\langle \frac{\gamma_i - \gamma}{\gamma_i + (d-1)\gamma} \right\rangle = 0 , \tag{1}$$

in which angular brackets denote averages over the conductance distribution $\rho_L(\gamma_i)$.

Thus our basic computational scheme for calculating the conductivity of disordered systems is the following: (1) Generate a cubic region of L^d sites, with site energies chosen at random from the site energy distribution function $\Gamma(\varepsilon_n)$ characterizing the disordered system of interest; (2) Calculate the conductance of this region for a given bulk carrier concentration (which we do using a numerically exact supercell procedure summarized in Sec. III); (3) Repeat this procedure for a sufficiently large number N_s of blocks, each one representing a randomly chosen cubic region of the actual disordered system, thereby accumulating a sample of conductances $\{\gamma_i\}$ representative of the distribution function $\rho_L(\gamma_i)$; and (4) Numerically find the root of Eq. (1) associated with this

conductance distribution. This means obtaining the root of the equation

$$\sum_{i=1}^{N_s} \frac{\gamma_i - \gamma}{\gamma_i + (d-1)\gamma} = 0 . \tag{2}$$

As we will show, the chief practical advantage of this idea over more traditional supercell calculations (which might simply approximate the bulk conductivity with the *direct average* of the block conductivity) is that the *effective-medium average* associated with Eqs. (1) and (2) is much less sensitive to the finite size of the blocks employed in the calculation. In this way, convergence to the infinite-system limit is obtained with a substantial savings in computer time and storage.

To put this general scheme into effect we need a way of computing the conductance of each block. This may be done in a number of different ways. In the next section we describe a general procedure which accomplishes this task for the physically important case in which the hopping rates connecting sites obey a well-defined detailed balance relation (which will be true for most systems of physical interest).

III. CALCULATION OF BLOCK CONDUCTANCES

A long-range random walk on an energetically disordered d-dimensional lattice can be described through the master equation

$$\frac{dP_s}{dt} = \sum_{s'} (F_{ss'} P_{s'} - F_{s's} P_s) , \tag{3}$$

in which $P_s(t)$ describes the probability of finding a particle at the site of lattice vector $s = (s_1, \ldots, s_d)$ at time t. (In what follows all distances are measured in lattice spacings.) The hopping rate

$$F_{ss'} = F(|s - s'|; \varepsilon_s, \varepsilon_{s'}) \tag{4}$$

from site s' to s is assumed to depend upon the distance $|s - s'|$ and upon the randomly and independently distributed energies ε_s and $\varepsilon_{s'}$ of the two sites involved in the transition. Because of this energy difference, the rates connecting two sites are not generally symmetric, i.e., forward and backward hopping rates are not generally equal. In most systems of physical interest, however, a detailed balance relation[22] of the form

$$F_{ss'} \rho(\varepsilon_{s'}) = F_{s's} \rho(\varepsilon_s) \tag{5}$$

relates forward and backward hopping rates to one another through the relative equilibrium probability $\rho(\varepsilon) = \rho(\varepsilon, \mu, T)$ of finding the particle at a site of energy ε. In most cases this equilibrium distribution function (which also determines the average carrier concentration in terms of the chemical potential μ and the temperature T) is unique and known *a priori* based upon the statistics (for example, Boltzmann or Fermi-Dirac) of the transport particles of interest. We assume this to be the case in what follows, although we will not need to specify the precise functional form that the distribution takes.

In keeping with the general procedure outlined in Sec.

II, our specific goal is to determine the transport properties associated with a particular cubic region, or block, having L sites along each edge. This is somewhat delicate, due to the possibility of long-range hops which might take a particle outside the original block. We circumvent this problem by replacing that part of the crystal surrounding the block of interest with identical copies of itself, infinite in number, identifying the diffusion tensor of each block with that of an infinite crystal that is periodically repeated from the original block in all directions. This new system is infinite in extent and invariant under translations T_L along crystal axes by multiples of the edge length L of the block, with each super-unit cell, or *supercell*, containing an identical random array of $N = L^d$ sites (see Fig. 2). Corresponding sites in each cell have the same energy $\varepsilon_s = \varepsilon_{s+L}$. The distance and energy dependence of hopping rates in the new infinitely-replicated system are assumed to be functionally identical to those in the original crystal, so that long-range rates extend, in principle, to all points in the new infinite system. Computationally, we seek a means for evaluating the diffusion constant for this new infinite system in terms of matrix manipulations performed on finite N-dimensional matrices. The equations of motion for the periodically repeated crystal can be written

$$\frac{dP_s^n}{dt} - \sum_{m,s'} W_{ss'}^{n,-m} P_{s'}^m = 0 , \tag{6}$$

in which P_s^n denotes the probability for the particle to be at lattice vector $r_s^n = (n + s)$ of the infinite system, and

$$W_{ss'}^m = F_{ss'}^m - \delta_{m,0} \delta_{ss'} \Omega_s , \tag{7}$$

where the superlattice vector (or supercell index) $n = (n_1, \ldots n_d)L$ locates the origin of the corresponding supercell, the $N = L^d$ intracell position vectors $s = (s_1, \ldots s_d)$ locate sites within each supercell, and we have defined

$$\Omega_s = \sum_{m,s'} F_{s's}^m . \tag{8}$$

In writing these expressions we have used translational invariance on length scale L to write the hopping rate connecting sites in different supercells

$$F_{ss'}^{mn} = F(|m + s - n - s'|; \varepsilon_s, \varepsilon_{s'}) = F_{ss'}^{m-n} \tag{9}$$

as a function of the supercell indices m and n only through the net displacement vector m-n connecting them.
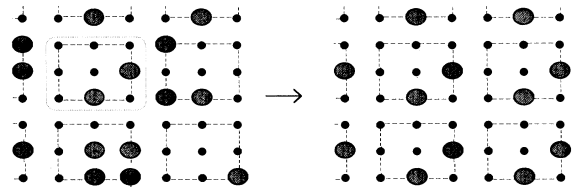

FIG. 2. To compute the equivalent conductance of a given super cell it is extracted from the disordered crystal and periodically repeated to form an infinite lattice which is translationally invariant on the scale of the supercell spacing.

In a recent publication,[11] we have shown how such a periodically repeated system can be mapped onto an "imaginary time" Schrödinger equation and the resulting equations solved to obtain an explicit spectral representation of the corresponding diffusion coefficient D. A straightforward extension of the work presented in that paper allows a similar expansion,

$$2d\, D_\nu = \langle \phi_0 | V_2^\nu | \phi_0 \rangle + 2 \sum_{\lambda \neq 0} \frac{|\langle \phi_0 | V_1^\nu | \phi_\lambda \rangle|^2}{\varepsilon_\lambda - \varepsilon_0} , \qquad (10)$$

to be obtained for the individual components D_ν of the diffusion tensor, in terms of the N eigenstates $\{|\phi_\lambda\rangle\}$ and eigenvalues ε_λ of an $N \times N$ "Hamiltonian" matrix H_0, and associated matrices V_1^ν and V_2^ν defined[11] through their matrix elements

$$\langle s | H_0 | s' \rangle = \sum_n H_{ss'}^n , \qquad (11a)$$

$$\langle s | V_1^\nu | s' \rangle = i \sum_m (m_\nu + s_\nu - s'_\nu) H_{ss'}^m , \qquad (11b)$$

$$\langle s | V_2^\nu | s' \rangle = \sum_m (m_\nu + s_\nu - s'_\nu)^2 H_{ss'}^m , \qquad (11c)$$

which, in turn, are defined in terms of a similarity transform

$$H_{ss'}^{mn} \equiv [\rho(\varepsilon_{s'})/\rho(\varepsilon_s)]^{1/2} W_{ss'}^{m-n} \qquad (12)$$

of the original transition matrix appearing in (7).

Equation (10) lends itself to an efficient computational scheme for computing the diffusion tensor associated with finite blocks of a given size L. A cubic region of this size containing a random distribution of site energies is generated in the computer and its transition matrix W and equilibrium populations $\rho(\varepsilon_s)$ determined. The matrix elements of the associated Hamiltonian H_0 and the operators V_1^ν and V_2^ν are then constructed using (11). [Although (11) implies an infinite sum over all supercells, it may be easily summed to numerical convergence for hopping rates which fall off with increasing separation.] This finite-dimensional Hamiltonian H_0 is then diagonalized numerically, and the resulting eigenvalues and eigenvectors used to evaluate the three Cartesian components D_ν of the diffusion tensor directly through (10) and (11). To compute the equilibrium (i.e., low field) conductance of the block we also need the local carrier concentration n_i. This is done by first determining the chemical potential μ and temperature T which, through the equilibrium distribution $\rho(\varepsilon, \mu, T)$ and site-energy distribution function $\Gamma(\varepsilon)$, determine the bulk carrier concentration

$$n = \int d\varepsilon\, \rho(\varepsilon, \mu, T) \Gamma(\varepsilon) \qquad (13)$$

of the material. The local carrier concentration is then easily computed using this value of μ and T through the relation

$$n_i = \sum_s \rho(\varepsilon_s, \mu, T) , \qquad (14)$$

where the sum now runs over the specific set of sites in the particular block under consideration. Thus, using the local components of the diffusion tensor and the local

carrier concentration we compute the components of a *block conductance* which we define through the relation

$$\gamma_i^\nu = \gamma_0 n_i D_i^\nu , \qquad (15)$$

where $\gamma_0 = e^2/kT$ is the usual combination of factors which relate the diffusion constant to the mobility. By computing this conductance for a sufficiently large number of randomly generated blocks we produce a reasonable sampling of the distribution $\rho(\gamma_i)$ of block conductances, which can then be used in conjunction with Eq. (2) to compute the bulk conductivity of the disordered system.

IV. APPLICATIONS TO BINARY LATTICES

To demonstrate the utility of the approach outlined in Secs. II and III we consider a number of applications involving *binary* lattices, i.e., systems in which lattice sites are randomly occupied by two types of site, so that the site-energy distribution function can be written

$$\Gamma(\varepsilon) = x\delta(\varepsilon - \varepsilon_1) + (1-x)\delta(\varepsilon - \varepsilon_2) . \qquad (16)$$

In the calculations that follow we consider only noninteracting carriers in fixed bulk carrier concentration n. In a future publication we intend to present calculations appropriate to interacting carriers (fermions), which incorporate the effect of site blocking on the conductivity, and to systems possessing a more extended site-energy distribution function.

A. Nearest-neighbor conduction on percolating lattices

As an initial example designed to test the robustness of the general approach, we have applied the method outlined in Secs. II and III to study the well-known problem of nearest-neighbor conduction on a site-percolating lattice.[2,16] For this problem we take x to be the fraction of conducting sites in the lattice (which we arbitrarily identify with sites of type ε_1), and choose the rates connecting *nearest-neighbor* sites on a three-dimensional cubic lattice as follows:

$$F(r; \varepsilon_i, \varepsilon_j) = [W_0 \delta_{ij} \delta_{i,1} + w(1 - \delta_{ij}\delta_{i,1})]\Theta(r - a) , \qquad (17)$$

with $W_{11} = W_0 \gg w = W_{22} = W_{12} = W_{21}$, and $\Theta(x)$ is the Heaviside step function. With this choice, nearest-neighbor pairs of type $i = j = 1$ are connected by large rates W_0, while nearest-neighbor pairs of any other type are connected by reduced rates w. This corresponds to a high-temperature limit in which all sites have the same equilibrium populations, since $W_{12}/W_{21} = 1$. It also represents an extension of the more common percolation problem in which the small (or less conducting) rate w is taken to be zero. Unfortunately, the transition matrix governing transport in the system becomes *decomposable* in the limit $w \to 0$, reflecting the existence of isolated clusters each of which tends individually towards its own equilibrium. This, of course, violates our initial assumption of a single equilibrium state for the entire lattice, and thus in the work presented here[24] we restrict ourselves to small but nonzero w. In spite of this limitation, with the small values we are able to use numerically the computa-

tional method does a respectable job of reproducing the conductivity of site-percolating lattices above the conduction threshold.

In Fig. 3 we present both linear and logarithmic plots of the conductivity versus the conducting site fraction x, normalized to unity at the conducting end. In this figure we compare results obtained using block sizes of edge length $L = 3$, 4, 5, and 6 to show the rapid convergence to the bulk limit that is obtained using our self-consistent large-cell renormalization approach. Each numerical data point for which the curve was calculated represents an effective-medium average over a set of 300 block conductances in which the magnitude of the "weak link" w was taken to be $10^{-8}W_0$, although only values of the conductivity above 10^{-6} are plotted to emphasize the percolative nature of the conductivity above the percolation threshold. In producing these curves we have kept the carrier concentration n fixed as a function of x, which

also keeps the carrier concentration *in the conducting region* itself constant as x is varied. This choice corresponds in the $w = 0$ limit to the standard site-percolation model.[2,16,18] A fit to the numerical data just above the transition region using a function of the form $\ln\sigma = t\ln(x - x_c)$ yields the values $x_c = 0.318$, which is in reasonable agreement with calculations performed on larger lattices, and the value $t = 1.47$, which is significantly lower than recent estimates $t > 1.8$ of the conductivity exponent.[23] This latter difference may arise from the finite value of the rate w that we have used in the calculations or from the finite-cell size used (an effect which will always become important in some immediate vicinity of the critical point).

B. Long-range conduction on site-percolating lattices

In Fig. 4 we present a set of curves similar to those in Fig. 3, except that we have removed the restriction to nearest-neighbor hopping. That is, we consider a binary lattice with exponentially decaying hopping rates having the functional form

$$F(r;\varepsilon_i,\varepsilon_j) = [W_0\delta_{ij}\delta_{i,1} + w(1 - \delta_{ij}\delta_{i,1})]\exp(-\alpha r) . \quad (18)$$

These curves were produced with a single cell size $L = 6$, again using 300 realizations per data point. Plotted curves correspond to values of the range parameter $\alpha = 2$, 10, 18, and 26. The dashed curve in that figure corresponds to nearest-neighbor transport, being the same as the corresponding curve for $L = 6$ in Fig. 3. Note the steady approach to a nearest-neighbor percolation-type transition in the neighborhood of $x = 0.3$ as the range $r_0 = \alpha^{-1}$ of the hopping rate decreases. Note also for $\alpha \geq 18$ the signature of a second-nearest-neighbor percolation transition between $x = 0.1$ and $x = 0.2$. The dropoff in this region with decreasing concentration is due, presumably, to the disappearance of a *second-*
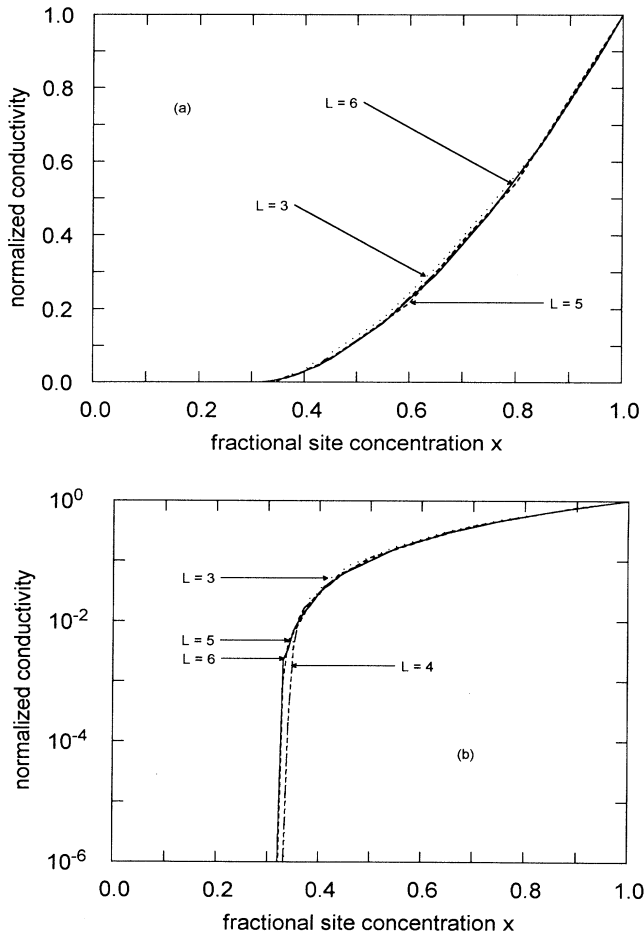

FIG. 3. Normalized conductivity as a function of the fractional conductive site concentration for a nearest-neighbor site-percolation-like problem, with supercell edge lengths of $L = 3$, 4, 5, and 6 sites. In the linear plot in (a) the dot-dashed curve for $L = 4$ is not discernible beneath the solid line representing $L = 6$. The difference becomes more apparent in the critical region when plotted on a logarithmic scale as in (b).
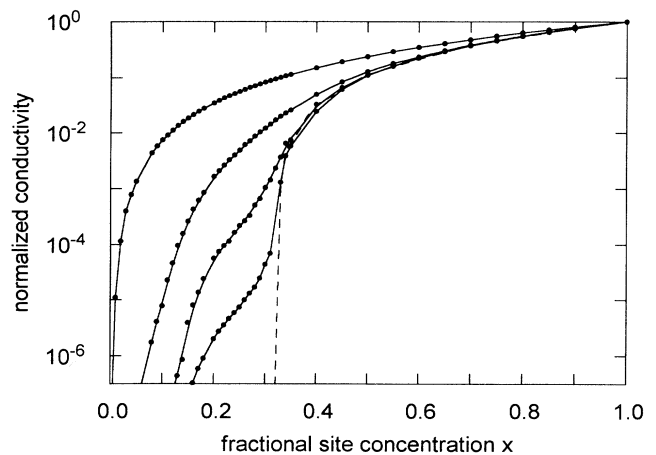

FIG. 4. Normalized conductivity as a function of the fractional conductive site concentration with variable-range hopping governed by exponential hopping rates. From upper-left to lower-right the curves presented correspond to values of the range parameter $\alpha = 2$, 10, 18, and 26. The dashed curve represents nearest-neighbor hopping only.

nearest-neighbor conducting path. This ability to reproduce greater-than-nearest-neighbor transition points recommends the accuracy of the basic computational approach.

C. Trapping-to-percolation crossover

A variation of the nearest-neighbor site-percolation problem, which may be more relevant to some physical systems, relaxes the high-temperature limit implicit in (17) by applying a detailed balance relation between the two different kinds of site. Thus, for the curves in Fig. 5 we have considered nearest-neighbor hopping with a hopping rate function given by the expression

$$F(r;\varepsilon_i,\varepsilon_j)=[\,W_1\delta_{i,1}\delta_{j,1}+w_{21}\delta_{i,2}\delta_{j,1}+W_2\delta_{i,2}\delta_{j,2}$$
$$+W_{12}\delta_{i,1}\delta_{j,2})]\Theta(r-a)\,,\qquad(19)$$

in which W_i is the hopping rate between neighboring pairs of sites of type ε_i, and in which there is a reduced rate w_{21} out of the (assumed lower energy) sites of type ε_1 when making hops to higher energy sites of type ε_2. Accordingly, we define the "well depth" $\eta=w_{21}/W_{12}=\exp[-\beta(\varepsilon_2-\varepsilon_1)]$ which provides a measure of the difference in site energies. In Fig. 5 we present calculations in which the well depth η is varied, while the rate between sites of the same type is kept fixed. Thus, in the curves presented, we take $W_1=W_2=W_{12}$, and $\eta=10^{-8}$, 10^{-5}, and 10^{-3}. For comparison, the dashed curve in this figure represents the nearest-neighbor site percolation curve, as in Fig. 3. The difference observed between the two curves above the percolation point is real and results from the fact that with different energies and a *fixed* bulk carrier concentration n, the relative concentration of carriers among the lower energy sites increases as the relative fraction of

lower energy sites decreases. That is, for large energy differences $\Delta=\varepsilon_2-\varepsilon_1$ most of the carriers end up in the lower energy states. This implies, for example, that for small x the relative carrier concentration among the few lower energy sites gets much larger than the bulk carrier fraction. Above the percolation threshold, by contrast, the carrier concentration in the percolating cluster decreases with increasing x towards that of the site percolation model, until they coincide at $x=1$.

These curves clearly show the effects of the trapping-to-percolation crossover that occurs in binary systems of this type.[9,10] For small x the carriers spend a great deal of time trapped in isolated clusters and sites of energy ε_2, making infrequent excursions among the higher energy sites. Conduction is then *trap limited*. At higher concentrations, above the percolation point x_c, carriers do not need to leave the lower energy manifold in order to participate in conduction. Thus a transition takes place between trap-limited and percolative conduction in this kind of system.

In Figs. 6 and 7 we present long range versions of the curves presented in Fig. 5, with exponential rates of the form

$$F(r;\varepsilon_i,\varepsilon_j)=[\,W_1\delta_{i,1}\delta_{j,1}+w_{21}\delta_{i,2}\delta_{j,1}+W_2\delta_{i,2}\delta_{j,2}$$
$$+W_{12}\delta_{i,1}\delta_{j,2})]\exp(-\alpha r)\,.\qquad(20)$$

In Fig. 6 we take the range parameter $\alpha=6$, and in Fig. 7 we take $\alpha=10$. In both curves the relative value of the parameters W_1, W_2, W_{12}, and η are the same as the corresponding curves in Fig. 5. While the same trapping behavior is seen at low concentrations, the transition which takes place occurs at lower concentrations as the effective hopping range $r_0=\alpha^{-1}$ is increased. It is interesting to note that the sharpness of the transition is not necessarily diminished with the increased range associated with exponentially decaying hopping rates.
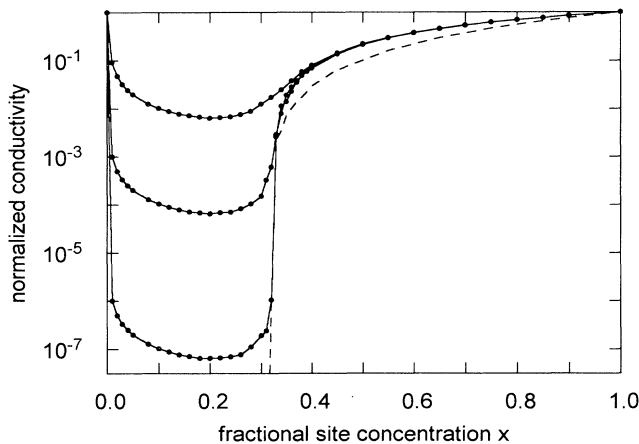

FIG. 5. Normalized conductivity as a function of the fractional concentration of deep energy sites with nearest-neighbor hopping. Note the trapping-to-percolation transition exhibited by these curves. End member conductivities are equivalent. Curves displayed correspond, from top to bottom, to a well depth $\eta=10^{-3}$, 10^{-5}, and 10^{-8}. Nearest-neighbor site percolation is shown as a dashed line.
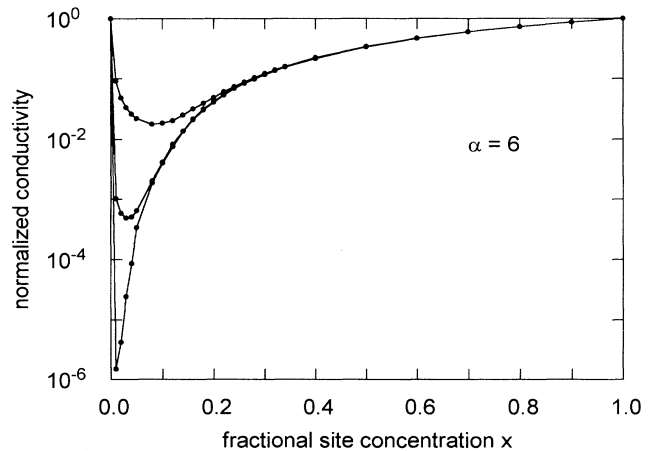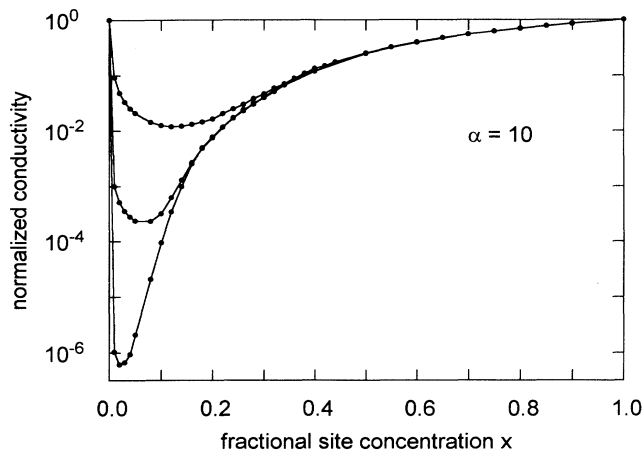

FIG. 6. Normalized conductivity as a function of the fractional concentration of deep energy sites for a system with exponential hopping rates, showing a trapping-to-percolation-like transition. In each of these curves the range parameter takes the value $\alpha=6$, while the well depth takes the values $\eta=10^{-3}$, 10^{-5}, and 10^{-8}, respectively, from top to bottom.

FIG. 7. Normalized conductivity as a function of the fractional concentration of deep energy sites for a system with exponential hopping rates, showing a trapping-to-percolation-like transition. In each of these curves the range parameter takes the value $\alpha = 10$, while the well depth takes the values $\eta = 10^{-3}$, 10^{-5}, and 10^{-8}, respectively, from top to bottom.
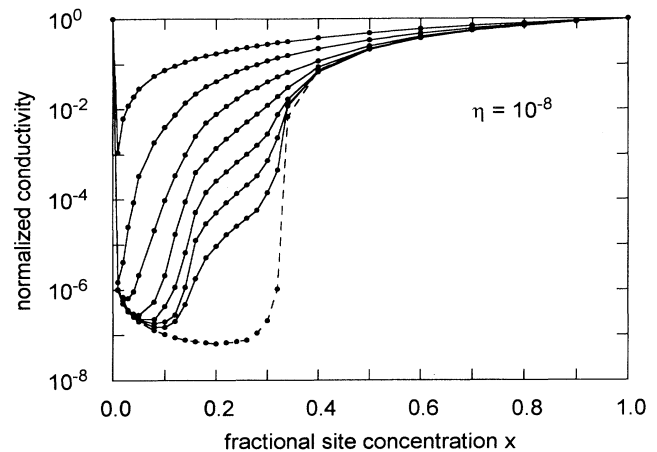
FIG. 8. Normalized conductivity as a function of the fractional concentration of deep energy sites for a system with exponential hopping rates, showing a trapping-to-percolation-like transition. In these curves the well depth $\eta = 10^{-8}$ is kept fixed, while the range parameter is varied over the values $\alpha = 2$, 6, 10, 14, 18, 22, and 26, respectively, from upper left to lower right. The dashed curve represents the nearest-neighbor trapping-to-percolation transition as depicted in Fig. 5.

As a final example of the method, we present a family of curves in Fig. 8 in which we fix the well depth $\eta = 10^{-8}$ and the range parameter α is varied from 2 to 26 with an increment of 4. Otherwise the rates are the same as in Fig. 5. The dashed line corresponds to the nearest-neighbor curve in Fig. 5 having the same well depth. It is interesting to note that the same kind of second-nearest-neighbor shoulders discussed in connection with Fig. 4 are also clearly evident in this plot.

V. SUMMARY

We have presented a general method for accurately calculating the conductivity of energetically disordered solids and demonstrated the approach on a series of model binary systems. The method works well on model calculations describing conduction on a site-percolating lattice and provides data for the trapping-to-percolation crossover to which analytical theories can be compared. In a future publication we will extend the formalism presented here to treat continuous site-energy distributions and interacting electrons. Further extensions of the method to treat systems in which topologically disordered hopping sites (i.e., not distributed on a lattice) are also currently under development and will be presented in a later publication.

ACKNOWLEDGMENT

[1]V. Ambegaokar, B. I. Halperin, and J. S. Langer, Phys. Rev. B 4, 2612 (1971).

[2]S. Kirkpatrick, Rev. Mod. Phys. 45, 574 (1973).

[3]H. Scher and M. Lax, Phys. Rev. B 7, 4491 (1973).

[4]H. Scher and M. Lax, Phys. Rev. B 7, 4502 (1973).

[5]L. Th. Pautmeier, J. C. Scott, and L. B. Schein, Chem. Phys. Lett. 197, 6 (1992).

[6]H. Bässler, Phys. Status Solidi B 175, 15 (1993), and references therein; Philos. Mag. B 50, 347 (1980); G. Schönherr and H. Bässler, ibid. 44, 47 (1981).

[7]P. Argyrakis and R. Kopelman, Phys. Rev. B 22, 1830 (1980); Chem. Phys. 57, 29 (1981); P. M. Borsenberger, L. Pautmeier, and H. Bässler, J. Chem. Phys. 94, 8 (1991).

[8]T. Holstein, Ann. Phys. (N.Y.) 8, 325 (1959); D. Emin and T. Holstein, ibid. 53, 439 (1969); D. Emin, Adv. Phys. 24, 305 (1975).

[9]R. Raffaelle, H. U. Anderson, D. M. Sparlin, and P. E. Parris, Phys. Rev. Lett. 65, 1383 (1990); Phys. Rev. B 43, 7991 (1991).

[10]P. E. Parris and B. D. Bookout, Phys. Rev. B 47, 562 (1993); 48, 9354 (1993).

[11]P. E. Parris and B. D. Bookout, Phys. Rev. Lett. 71, 16 (1993).

[12]D. L. Huber, in Excitation Dynamics in Molecular Solids, Topics in Applied Physics Vol. 49, edited by W. M. Yen and P. M. Selzer (Springer-Verlag, Berlin, 1981); Phys. Rev. B 20, 2307 (1979); 20, 5333 (1979).

[13]J. Klafter and R. Silbey, Phys. Rev. Lett. 44, 55 (1980); J. Chem. Phys. 72, 843 (1980); J. Klafter and M. F. Shlesinger, Proc. Nat. Acad. Sci. USA 83, 848 (1986).

[14]A. Blumen, J. Klafter, and R. Silbey, J. Chem. Phys. 72, 5320 (1980); A. Blumen, ibid. 72, 2632 (1980); A. Blumen and J. Manz, ibid. 71, 4694 (1979); R. F. Loring, H. C. Anderson, and M. D. Fayer, ibid. 76, 2015 (1982); Phys. Rev. Lett. 50,

1324 (1983); C. R. Gochanour, H. C. Anderson, and M. D. Fayer, J. Chem. Phys. **70**, 4254 (1979).

[15]K. W. Kehr and K. Binder, in *Applications of the Monte Carlo Method in Statistical Physics,* Topics in Current Physics Vol. 36, edited by K. Binder (Springer, Berlin, 1987), and references therein.

[16]D. Stauffer, *Introduction to Percolation Theory* (Taylor & Francis, London, 1985), pp. 70–89.

[17]S. Alexander, J. Bernasconi, W. R. Schneider, and R. Orbach, Rev. Mod. Phys. **53**, 175 (1981).

[18]B. D. Hughes, in *The Mathematics and Physics of Disordered Media,* edited by B. D. Hughes and B. W. Ninham (Springer-Verlag, Berlin, 1983); M. Sahimi, B. D. Hughes, L. E. Scriven, and H. T. Davis, J. Chem. Phys. **78**, 6849 (1983).

[19]J. W. Haus and K. W. Kehr, Phys. Rep. **150**, 265 (1987), and references therein.

[20]T. Odagaki and M. Lax, Phys. Rev. B **25**, 2301 (1982); **24**, 5284 (1981); T. Odagaki, M. Lax, and A. Puri, *ibid.* **28**, 2755 (1983).

[21]P. E. Parris, Phys. Rev. B **36**, 5437 (1987); **40**, 4928 (1989).

[22]General properties of master equations obeying detailed balance are discussed in some detail by N. G. van Kampen, *Stochastic Processes in Chemistry and Physics* (North-Holland, Amsterdam, 1981), pp. 101–135.

[23]Muhamid Sahimi, in *The Mathematics and Physics of Disordered Media,* edited by B. D. Hughes and B. W. Ninham (Springer-Verlag, Berlin, 1983).

[24]It is straightforward to extend the present approach to calculate the conductivity of a percolating lattice with $w=0$. To do this requires only that the sites belonging to the percolating cluster spanning each cell (should one exist) be identified, so that the transition matrix could then be produced only for the connected set of sites within the percolating cluster (which will have its own unique equilibrium state). The diffusivity/conductivity of the (periodically repeated) percolating cluster could then be obtained in the manner described above.